DEVIATION FROM DARCY'S LAW: AN IMPLICATION OF UNSATURATED FLOW IN DUAL-SCALE FIBER MATS IN LCM

Murthy S. Munagavalasa[1] and Krishna M. Pillai[2]

[1]S.C. Johnson & Son, Inc., 1525 Howe Street, Mail Station 153, Racine, WI 53403-2236, USA: MSMunaga@SCJ.COM

[2]Department of Mechanical Engineering, University of Wisconsin- Milwaukee, Milwaukee, WI 53201, USA: krishna@uwm.edu

ABSTRACT: Liquid Composite Molding (LCM) processes including RTM and VARTM are used for producing polymer matrix composite. In any typical LCM process a thermoset resin is injected/sucked into a mold cavity with a pre-placed preform of fiber mats. The dual-scale nature of those fiber preforms gives rise to the unsaturated flow during mold filling in LCM processes that is characterized by a modified continuity equation with a `sink' term due to the delayed absorption of resin by fiber tows behind the flow front. Application of the mathematically rigorous volume averaging method results in a momentum balance equation that has two additional terms apart from the pressure gradient terms associated with the Darcy's law. In this paper, we would explore the importance of these two terms (called the Brinkman term and the interfacial kinetic-effect tensor term) near the flow front in a dual-scale porous medium created by the dual-scale fiber mats. Through a numerical simulation of the unsaturated flow in an idealized dual-scale porous media, it is discovered that these two terms become significant in a small region behind the flow front where the sink term changes rapidly. So the results suggest that a modified form of Darcy's law needs to be used near the flow front during LCM mold-filling simulation in a dual-scale fiber mat.

KEYWORDS: RTM, resin transfer molding, LCM, liquid composite molding, unsaturated flow, Darcy's Law, polymer composites, dual-scale porous media

INTRODUCTION

Composite materials have become critically important in aerospace, automotive, and civil engineering areas along with the biomechanics and other fields because of their high stiffness to weight ratio, long fatigue life, increased corrosion resistance, and their ability to consolidate parts. Liquid composite molding (LCM) technologies such as the resin transfer molding (RTM), vacuum assisted RTM (VARTM), and Seeman Composite Resin Infusion Molding Process, are very important in the manufacture of polymer composites [1]. These composites consist of polymeric matrix which is interspersed with reinforcements such as carbon and glass fibers. In LCM, the composites are created by impregnating a fiber-packed mold cavity with resin by injecting it through the inlet gates of the mold. Numerical simulation of such mold-filling process in LCM is becoming indispensable for optimizing the mold design [2-5].

An LCM mold containing randomly oriented fibers of a random mat is an example of the single-scale porous medium. Here, all the pores are of the same length-scale. The fibers are impermeable and the spacing between fibers can be treated as homogeneous. However, if the

solid phase is porous with the pore size of a much smaller length-scale, the porous medium is then classified as a dual length-scale or dual porosity porous medium. Braided, woven or stitched fiber mats used in LCM processes, where fiber bundles are permeable to resin due to presence of pores between fibers within the bundles, fall under this category. The transport processes that occur inside this dual-scale porous medium are often significantly different from that of the single-scale porous medium. Babu and Pillai [6] discovered that the dual-scale porous media with continuous inter-tow gaps[1] (created by the stitched mats only) allow the lead-lag flow to manifest where the resin races along the gaps before fully impregnating the tows[2]. The delayed wetting of tows behind the resin front in the gap region leads to a region of partial saturation behind the front in such dual-scale fiber mats. The flow in such a region is called the *unsaturated* flow and is often characterized either by a visually observable region of a lighter hue as compared to the darker saturated region, or by a droop in the inlet-pressure history [6]. The onset of the unsaturated flow the dual-scale stitched mats can be predicted by certain dimensionless numbers such as the pore volume ratio and sink effect index [8]. A synopsis of some recent work on the unsaturated flow in dual-scale porous media was presented by Roy et al. [7].

Mathematically rigorous volume averaging method have been adopted to derive the averaged form of mass and momentum equations for the unsaturated flow in dual-scale porous media encountered during mold filling in LCM processes [9,17]. During the averaging process, averaging of the shear stress term of the Navier-Stokes equation in the gap region gives rise to a new quantity named the *interfacial kinetic-effects* tensor which includes the effects of liquid absorption by the tows, and the presence of slip velocity on their surface. Initial scaling analysis suggested that its effect on the momentum balance becomes negligible if the gradient of the rate of resin absorption by the tows is small [9]. However, beyond this qualitative insight, no estimate of the magnitude of this newly found term is available in the literature nor have we encountered any studies wherein the effect of spatial variation of the absorption rate on this term is discussed.

The objective of this work is to estimate the magnitude of two forces that results due to 1) the interfacial kinetic-effects at the tow-gap interface (the *interfacial kinetic-effects* force), as well as 2) the deceleration of the average velocity (the *Brinkman* force) in the unsaturated region of isothermal flow in a dual-scale porous medium. A finite element based numerical method is used to model 2-D isothermal unsaturated flow between two parallel porous plates. Parametric studies are conducted to evaluate the two forces in the unsaturated region just behind the flow front.

Summary of volume averaged transport equations

Pillai [9] rigorously derived the macroscopic transport equations for isothermal flow in the dual-scale porous media using the volume averaging method, the summary of which is presented in this section. Only the relevant gap-averaged balance laws will be listed; their derivation as well as the estimation of their various source and sink terms with the help of the single-scale model for the intra-tow flows is presented elsewhere [9].

Flow variables in LCM are invariably averaged in an averaging volume called REV or the representative elementary volume. For the fibrous dual-scale porous media, Pillai [9,17] has proposed an REV shown in Fig. 1 where the averaging volume consists of the gap and tow regions.

[1] Large-scale pores between tows will be referred to as the gap phase or gap region, or just gaps.
[2] Fiber bundles will be referred to as the tow phase or tow region, or just tows.

Mass balance equation for macroscopic flow in the gap region is given as

$$\nabla \cdot \left\langle \mathbf{v}_g \right\rangle = -S \tag{1}$$

Here $\left\langle \mathbf{v}_g \right\rangle$ is the volume-averaged liquid velocity in the inter-tow gaps, and is computed as $\left\langle \mathbf{v}_g \right\rangle = 1/\mathrm{V} \int_{\mathrm{V}_g} \mathbf{v}_g \mathrm{dV}$ where, as shown in Fig. 1, V and $\mathrm{V_g}$ are the total and the gap volumes for the REV. (Subscript g indicate quantities that are of the gap region.) *S* is the sink term and is equal to the volumetric rate of absorption of resin by the tows per unit volume as

$$\mathrm{S} = \frac{1}{\mathrm{V}} \int_{\mathrm{A_{gt}}} \mathbf{v}_\mathrm{g} \cdot \mathbf{n}_\mathrm{gt} \mathrm{dA} \tag{2}$$

where $\mathrm{A_{gt}}$ is the gap-tow interface area within the REV, and $\mathbf{n}_\mathrm{gt}$ is the unit normal at the gap-tow interface directed from gaps to tows.

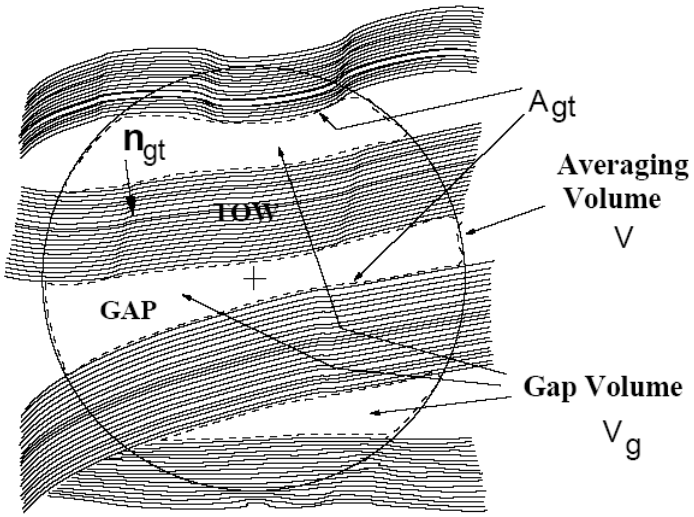

Fig.1. A typical Representative Elementary Volume (REV), or the averaging volume, for a fibrous dual-scale porous medium

The minus sign of the sink term in the continuity equation (1) suggests that the flow of the resin slows down in the unsaturated gap region because of the absorption of resin by fiber tows. An estimation of S requires the integration of resin flux into the tows, which in turn require solving the single-scale transport equations within the tow region [7,17].

Momentum balance equation for the gap region is derived to be

$$-\varepsilon_g \nabla \left\langle \mathrm{P}_g \right\rangle^g + \mu_g \left\{ \nabla^2 \left\langle \mathbf{v}_g \right\rangle + \nabla \cdot \mathbf{I} \right\} - \varepsilon_g \mu_g \mathbf{K}_\mathrm{g}^{-1} \cdot \left\langle \mathbf{v}_g \right\rangle = 0 \tag{3}$$

where $\varepsilon_\mathrm{g} = \mathrm{V_g} / \mathrm{V}$ is the gap volume fraction, $\left\langle \mathrm{P}_g \right\rangle^g$ is the gap-averaged resin pressure computed as $\left\langle \mathrm{P}_g \right\rangle^g = 1/\mathrm{V_g} \int_{\mathrm{V}_g} \mathrm{P}_g \mathrm{dV}$, μ_g is the viscosity of resin flowing in the gaps, and $\mathbf{K}_\mathrm{g}$ is the permeability tensor for flow in the gaps. **I**, the *interfacial kinetic-effects* tensor, is defined as

$$\mathbf{I} = -\mathrm{S}\delta + \frac{1}{\mathrm{V}} \int_{\mathrm{A_{gt}}} \left(\mathbf{v}_\mathrm{g} \mathbf{n}_\mathrm{gt} + \mathbf{n}_\mathrm{gt} \mathbf{v}_\mathrm{g} \right) \mathrm{dA} \tag{4}$$

with δ as the unit tensor. Note that $\mathbf{I}$ becomes identically equal to zero when the tows are impermeable. (Since $\mathbf{v}_g$ on gap tow interface becomes zero due to the no-slip condition on the solid tows.).

Eq. (3) is the dual-scale equivalent of the Brinkman's equation for single-scale porous medium [10]. This equation differs from that for single-scale porous medium in that the later equation does not contain the term $\mu_g \nabla \cdot \mathbf{I}$, which we would name as the *interfacial kinetic-effect force*[3], and which is likely to decelerate the gap flow in the regions of extreme gradients in the sink function S that take place very close to the flow front. The first term $-\varepsilon_g \nabla \langle P_g \rangle^g$ is the pressure force which drives the macroscopic gap flow. The second term $\mu_g \nabla^2 \langle \mathbf{v}_g \rangle$, which is to be called the *Brinkman force*, also tends to slow down the flow and becomes significant in areas of large changes in the gradients of the volume averaged velocities, such as at the interface of a dual-scale porous medium adjoining an open channel (section 2.11 in Ref. [14]). The last term $-\varepsilon_g \mu_g \mathbf{K}^{-1} \cdot \langle \mathbf{v}_g \rangle$ represents the net force at the solid-fluid interface.

ANALYZING FLOW IN A UNIDIRECTIONAL DUAL-SCALE MEDIUM

We study the unsaturated flow behind a resin front that is moving through an idealized unidirectional fiber mat, and which is represented as a set of parallel channels of width l_o (representing gaps in the dual-scale medium) separated by porous tows of thickness l_i each. (See Fig. 2A.) A target unit cell consisting of several thin REVs (Fig. 2B) is selected to conduct flow simulation in the gap region. The target unit cell is preceded by a hypothetical precursor unit cell, which is there merely to provide a realistic inlet velocity condition to the former. An exponentially increasing gap-to-tow `sink' velocity, along with a Beavers-Joseph slip velocity is imposed within the unit cell at the gap-tow interface [15]. The resultant flow field is used to estimate the non-Darcy terms in the gap-averaged momentum balance equation and evaluate their importance.

Reformulating the momentum balance equation

We now rearrange Eq. (3) to obtain an equation similar to Darcy's Law. Contracting both sides of Eq. (3) by taking a dot product with $\mathbf{K}_g$ and dividing both sides by $\varepsilon_g \mu_g$, we get

$$\langle \mathbf{v}_g \rangle = -\frac{\mathbf{K}_g}{\mu_g} \cdot \nabla \langle P_g \rangle^g + \frac{\mathbf{K}_g}{\varepsilon_g} \cdot \nabla^2 \langle \mathbf{v}_g \rangle + \frac{\mathbf{K}_g}{\varepsilon_g} \cdot (\nabla \cdot \mathbf{I}) \tag{5}$$

This equation can be regarded as a Darcy's Law with two correction terms: the first arising from the Brinkman force and the second from the interfacial kinetic-effect force. Retention of these two terms depends on how significant these terms are in the unsaturated region just behind the moving resin front.

Non-dimensionalizing Eqn. (5) and taking its x-component (see [15] for details) results in

[3] Note that all terms in Eqn. (3) has the dimensions of force per unit volume.

$$\left\langle v_g^{\,*}\right\rangle_x = -\frac{K_{g,xx}^{\,*}}{\mu_g^{\,*}}\frac{\partial\left\langle P_g^{\,*}\right\rangle^g}{\partial x^*} + \frac{K_{g,xx}^{\,*}}{\varepsilon_g}\frac{\partial^2\left\langle v_g^{\,*}\right\rangle_x}{\partial x^{*2}} - \frac{K_{g,xx}^{\,*}}{\varepsilon_g}\frac{\partial S^*}{\partial x^*} \tag{6}$$

Superscript * represents dimensionless quantities. The y-component of Eq. (5) is also satisfied as its both sides become identically equal to zero. After exploiting the inherent symmetries in the posed flow problem, Eq. (6) can be reorganized further [15] as

$$\left\langle v_g^{\,*}\right\rangle_x = -\frac{K_{g,xx}^{\,*}}{\mu_g^{\,*}}\frac{\partial\left\langle P_g^{\,*}\right\rangle^g}{\partial x^*}\left(1 - R_B - R_I\right) \tag{7}$$

where R_B, to be referred to as *Brinkman correction factor*, is the dimensionless ratio of Brinkman force to pressure force:

$$R_B = \frac{\mu_g^{\,*}}{\varepsilon_g}\left(\frac{\partial^2\left\langle v_g^{\,*}\right\rangle_x}{\partial x^{*2}}\right)\Bigg/\left(\frac{\partial\left\langle P_g^{\,*}\right\rangle^g}{\partial x^*}\right) = \mu_g^{\,*}\left(\frac{\partial^2\left\langle v_g^{\,*}\right\rangle^g{}_x}{\partial x^{*2}}\right)\Bigg/\left(\frac{\partial\left\langle P_g^{\,*}\right\rangle^g}{\partial x^*}\right) \tag{8}$$

In the above equation, $\left\langle v_g^{\,*}\right\rangle_x / \varepsilon_g$ is replaced by $\left\langle v_g^{\,*}\right\rangle_x$[4].

R_I, to be called the *interfacial kinetic- effect correction factor*, is the dimensionless ratio of interfacial kinetic-effect force to pressure force:

$$R_I = -\frac{\mu_g^{\,*}}{\varepsilon_g}\left(\frac{\partial S^*}{\partial x^*}\right)\Bigg/\left(\frac{\partial\left\langle P_g^{\,*}\right\rangle^g}{\partial x^*}\right) \tag{9}$$

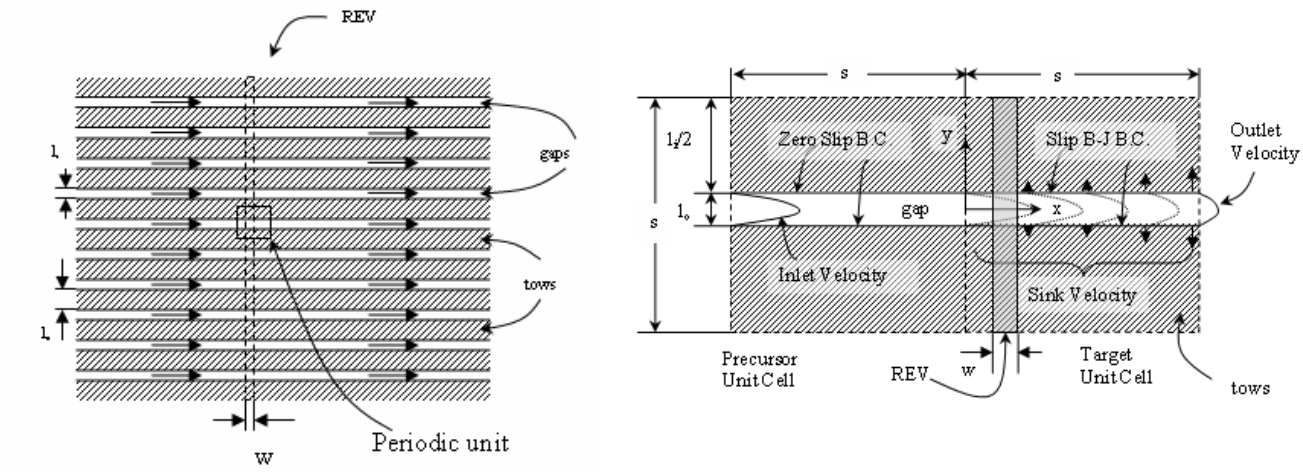

Part A Part B

Fig. 2. Part A: Schematic of a 2-D resin flow through gaps in a bank of porous and liquid absorbing 2-D tows (with infinite depth) stacked parallel to each other. The REV shown here is a thin disc of infinite width and a finite x-direction length 'w'. Part B: Exploded view of the periodic target unit cell of size 's' shown in Part A along with the hypothetical precursor unit cell. The sink velocity and slip boundary conditions exist only in target unit cell. Parabolic velocity profile is assumed at the entrance of the precursor unit cell.

[4] Note that ε_g being constant for our medium shown in Fig. 2 enables it to be moved inside the double derivative.

Flow simulation

A finite element based multiphysics software COMSOL Multiphysics 3.2 [16] is used to solve the point wise continuity and momentum balance equations in the gap region. Typical parameter values used in this simulation as well as other details are listed elsewhere [15]. The dimensionless velocity at the precursor cell inlet is assumed to be parabolic to resemble the fully developed flow through parallel plates and the dimensionless inlet velocity averaged over the inlet area is taken as unity. The interface between the two unit cells is treated as an internal boundary condition. Both the Beavers-Joseph slip boundary condition and variable sink velocity in the direction of flow is considered in the analysis.

Traditional volume averaging method, which requires that the representative elementary volume (REV) be of the same size as the unit cell, cannot be applied here as the effect of rapidly changing sink velocity on the correction terms will be lost. Instead, a specialized form of volume averaging method is adopted where the unit cell is subdivided into thin slices of REVs within which, the averaging of flow quantities is carried out. The width of these subdivided slices are one-tenth of that of the target unit cell throughout the unit cell except near the exit where the width is reduced to one-hundredth [15]. The much finer slicing of the unit cell closer to the flow front ensures that the volume averaged quantities (especially the absorption rate) are sufficiently accurate even in regions where the sink gradients are high.

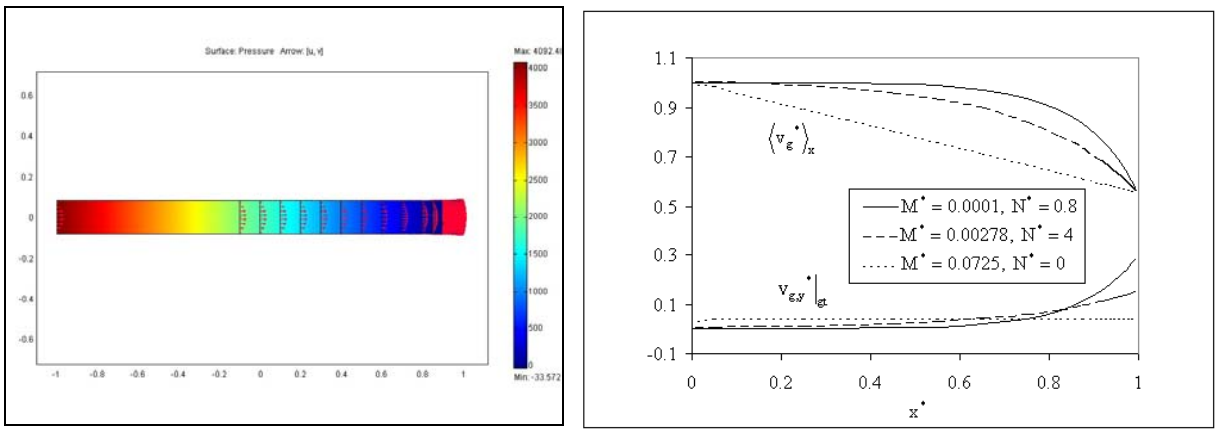

Part A Part B

Fig. 3 Part A: A COMSOL Multiphysics 3.2 schematic of pressure and velocity profiles in precursor and target unit cells. The smaller cells on the right hand side are within the target unit cell ($0 \le x^* \le 1$) and represent the sliced REVs. Part B: Various absorption rates at the gap-tow interface (the lower curves) within the target unit cell and the corresponding volume averaged velocity distributions (the upper curves).

Once the microscopic transport equations are solved (Fig. 3(A) describes a typical distribution of point wise velocity and pressure), macroscopic quantities such as $\left\langle v_g^* \right\rangle_x$ and $\left\langle P_g^* \right\rangle^g$ are computed for each REV slice by integrating the local velocity and pressure. Later the derivatives of these quantities are estimated through the backward differencing schemes such that each node value corresponds to the average at the REV slice.

RESULTS, DISCUSSION AND CONCLUSION

The gap-tow absorption velocity or the sink term as a function of x-coordinate is changed by varying parameters M^* and N^* of an exponential function $[v_{g,y}|_{gt} = M^* \exp(N^* x^*)]$ as shown in Part B of Fig. 3B such that the area under the curves remains the same in order to maintain constant outlet velocity. This figure also shows the variation of the volume-averaged x-velocity as a function of x^* confirming that the outlet velocity, and hence the total absorption rate within the unit cell, remains constant for all absorption rates considered.

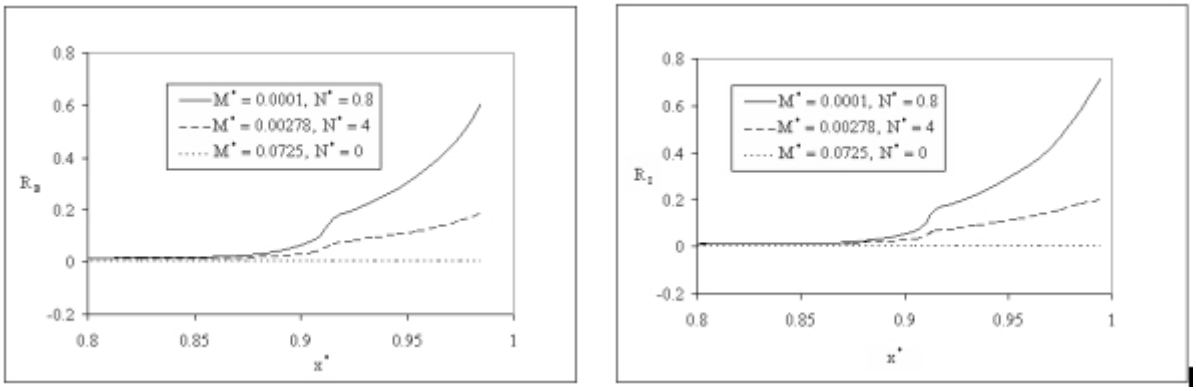

Part A Part B

Fig. 4 The Brinkman (RB) and interfacial kinetic-effect (RI) correction factors as a function of x^* are plotted in Parts A and B at various absorption rates.

Part A and B of Fig. 4 show R_B and R_I as functions of x^*. The plot indicates that both R_B and R_I are proportional to the gradient of the sink term. The *Brinkman correction factor* can reach a value as high as 0.6 and the *interfacial kinetic-effect correction factor* can reach values up to 0.7. For those tows that are directly behind the flow front where the absorption gradient is steep[5], the *Brinkman* and *interfacial kinetic-effect correction factors* become significant and hence cannot be discarded in the flow analysis unlike in fully saturated region. Although this means that unsaturated flow modeling is complicated near the flow front due to a large gradient in the sink term, this finding is of fundamental importance and suggests the retention of the correction factors R_B and R_I for accurate modeling of LCM processes.

See [15] for a description of dependence of R_B and R_I on the local Reynolds number, the slip velocity, and the slip coefficient.

After studying this interesting result, we can finally conclude that the hitherto neglected Brinkman and the interfacial kinetic-effect tensor terms in the momentum balance equation will become important in a small region just behind the resin front in a dual-scale fiber mat (especially the unidirectional one) due to a strong gradient in the sink term.

[5] The velocity of the flow front within the tow is inversely proportional to the extent of penetration of the flow front from the tow-gap interface. Since the tows directly behind the flow front in the gap region are just exposed to the resin, the extent of penetration is minimal and hence the gradient of absorption rate is very steep.

REFERENCES

[1] Rudd, C.D., Long, A.C., Kendall, K.N. and Mangin, C.G.E., *Liquid molding technologies*, Woodhead Publishing Ltd, 1997.

[2] Bruschke, M.V. and Advani, S.G., *RTM filling simulation of complex three dimensional shell-like structures*, SAMPE Q, Vol. 23(1), pp. 2-11, 1991.

[3] Fracchia, C.A., Castro, J. and Tucker III, C.L., A finite element/control volume simulation of resin transfer molding, *Proceedings of the American Society for Composites Fourth Tech. Conf.*, pp. 157-66, 1989.

[4] Fong, L.U., Varma, R.R., Liu, B., Bruschke, M.V. and Advani, S.G., *LIMS user's manual*, Centre for Composite Materials, University of Delaware, Newark, 1993.

[5] Moldflow Plastics Insight®, Moldflow Corporation (http://www. moldflow.com/), Lexington, MA.

[6] Babu, B.Z. and Pillai, K.M., Experimental investigation of the effect of fiber- mat architecture on the unsaturated flow in liquid composite molding, *J. of Compos. Mater.,* Vol. 38(1), pp. 57-79, 2003.

[7] Roy, T., Babu, B.Z., Jadhav, R.S., Munagavalasa, M.S. and Pillai, K.M., Some studies on modeling the unsaturated flow in woven, stitched or braided fiber mats in LCM, *Proceedings of the 7th Int. Conf. on Flow Processes in Comp. Mater. (FPCM7)*, Newark, 2004.

[8] Roy, T. and Pillai, K.M., Characterization of dual-scale fiber mats for unsaturated flow in liquid composite molding, *Polymer Composites*, Vol. 26(6), pp. 756-769, 2005.

[9] Pillai, K.M., Governing equations for unsaturated flow through woven fiber mats. Part 1. Isothermal flows, *Composites Part A*, Vol. 33, pp. 1007-1019, 2002.

[10] Tucker III, C.L. and Dessenberger, R.B., Governing equations for flow and heat transfer in stationary fiber beds, *Flow and rheology in polymer composites manufacturing*, Elsevier, Amsterdam, pp. 257-323, 1994.

[11] Bear, J. and Bachmat, Y., *Introduction to modeling of transport phenomena in porous media*, Kluwer Academic Publishers, Dordrecht, 1990.

[12] Whitaker, S., *The Method of Volume Averaging*, Kluwer Academic Publishers, Dordrecht, 1999.

[13] Slattery, J.C., *Single-phase flow through porous media*, AIChE J, Vol. 15(6), pp. 866-72, 1969.

[14] Kaviany, M., *Principles of heat transfer in porous media*, Springer, New York, 1995.

[15] Munagavalasa, M.S. and Pillai, K.M., Deviation from Darcy's Law: an implication of unsaturated flow in dual-scale porous media, manuscript to be submitted to *Journal of Porous Media* for publication.

[16] Comsol Multiphysics®, Comsol, Inc. (http://www.comsol.com), Los Angeles, CA.

[17] Pillai, K.M., and Munagavalasa, M.S., Governing equations for unsaturated flow through woven fiber mats. Part 1. Nonisothermal reactive flows, *Composites Part A*, Vol. 35, pp. 403-415, 2004.